RSC Advances

This is an *Accepted Manuscript*, which has been through the Royal Society of Chemistry peer review process and has been accepted for publication.

Accepted Manuscripts are published online shortly after acceptance, before technical editing, formatting and proof reading. Using this free service, authors can make their results available to the community, in citable form, before we publish the edited article. This *Accepted Manuscript* will be replaced by the edited, formatted and paginated article as soon as this is available.

You can find more information about *Accepted Manuscripts* in the Information for Authors.

Please note that technical editing may introduce minor changes to the text and/or graphics, which may alter content. The journal's standard Terms & Conditions and the Ethical guidelines still apply. In no event shall the Royal Society of Chemistry be held responsible for any errors or omissions in this *Accepted Manuscript* or any consequences arising from the use of any information it contains.

ROYAL SOCIETY OF CHEMISTRY

www.rsc.org/advances

A novel and highly sensitive gaseous n-hexane sensor based on thermal desorption/cataluminescence

Jianzhong Zheng [a], Wuxiang Zhang [a], Jing Cao [b], Xuehong Su [a], Shaofang Li [a], Shirong Hu [a], Shunxing Li [a], Zhiming Rao*[a]

(Jianzhong Zheng and Wuxiang Zhang contributed equally to this work.)

[a]*College of Chemistry and Environmental Science, Minnan Normal University, Zhangzhou 363000, P. R. China*

[b]*College of Chemistry and Chemical Engineering, University of Chinese Academy of Sciences, Beijing 100049, P. R. China*

* To whom correspondence should be addressed. Tel: +86 596 2591445, Fax: +86 596 2520035, E-mail: raozhm1944@126.com.

RSC Advances Accepted Manuscript

Abstract

A novel and highly sensitive sensor for gaseous n-hexane utilizing the sensing material Y_2O_3-Al_2O_3 (mass ratio of 2:1) has been developed based on the thermal desorption/cataluminescence (TD/CTL). Firstly, the cataluminescence characteristics of the above sensor have been investigated. Then, the optimal conditions of the developed sensor for the determination of n-hexane have been analyzed using response surface methodology (RSM). When the sensor was performed at the optimal catalytic temperature (Tc) of 200 ^{o}C and the wavelength of 400 nm, the linear range was 1.32-132 mg/m^3 with the detection limit of 0.4 mg/m^3. In addition, there was little to no response when contaminating volatile substances including benzene, toluene, chloroform, ethanol, and cyclohexane was passed through the sensor. This proposed TD/CTL-based n-hexane sensor shows high sensitivity, good stability, and rapid response and allows real time monitoring of n-hexane in air.

1. Introduction

Human exposure to n-hexane is relatively frequent as it is widely used in many industries as a solvent and thinner. However, occupational exposure to n-hexane may induce some neurotoxic effects; for example, n-hexane is metabolized to 2, 5-hexanedione, which is the neurotoxic agent and the indicator chosen for the biological monitoring of exposed

RSC Advances Accepted Manuscript

workers.[1-4] In addition, as a major indoor and industrial air pollutant, n-hexane has been recommended as one of the eight representative indoor volatile organic compounds (VOCs). Recently, considerable effort has been made to protect against significant negative effects of air pollution to human health and the environment.[5-7] Thus, the hazardous properties of n-hexane make monitoring it in air necessary and important.

Thus far, the methods for determining n-hexane in air are mainly gas chromatography spectrometry (GC), gas chromatography-mass spectrometry (GC/MS) and cataluminescence (CTL.) However, GC[8] and GC/MS[9] are typically clumsy, complicated, and expensive to manufacture. Worse still, GC and GC/MS use poisonous carbonyl disulfide or benzene as the solvent, which do harm to human health. Recently, CTL has attracted widespread attention in the field of gas sensors owing to their advantages of simplicity, rapid response and solvent-free.[10-25]

P. Yang, etc[13] proposed a CTL-based n-hexane sensor, and the linear range of CTL intensity versus concentration of n-hexane was 776-23280 mg/m^3 with a detection limit of 155 mg/m^3. However, the hygienic standard for n-hexane in air of residential area is 60 mg/m^3 (GB 18057-2000, China). Obviously, the sensitivity of CTL-based n-hexane sensor isn't high enough, and this kind of n-hexane sensor is unsuitable for the quality monitoring of n-hexane in air.

Response surface methodology (RSM), a collection of mathematical

RSC Advances Accepted Manuscript

and statistical techniques, useful for analyzing the effects of several independent variables on the response, is the most popular optimization method and has been successfully used in chemical process.[26-28] Herein, by using this method, the optimal conditions of the sensor for the determination of n-hexane were investigated.

In this paper, a novel and highly sensitive n-hexane sensor utilizing the sensing material Y_2O_3-Al_2O_3 (mass ratio of 2:1) based on the thermal desorption/cataluminescence (TD/CTL) has been designed. γ-Al_2O_3 has been widely used as oxidic supports in some reports.[29-32] However, thus far, to our knowledge, no reports on the use of Y_2O_3/Al_2O_3 as catalyst have been published so far. Moreover, we find that Y_2O_3-Al_2O_3 (mass ratio of 2:1) have shown the highest CTL intensity and better selectivity to n-hexane than other materials in our experiments. Furthermore, we have chosen an appropriate adsorbent (Tenax-TA) to improve the selectivity of this method. Using the adsorbent (0.12 g, in an adsorption tube) by air sampler, the trace n-hexane vapor in air is enriched. Owing to the tiny volume of the adsorption tube, the concentration of the desorbed n-hexane is much higher than former concentration in the air, so the sensitivity of TD/CTL-based sensor is much higher than CTL-based sensor, with a lower detection limit of 0.4 mg/m^3 compared to that without adding TD (8 mg/m^3). This TD/CTL-based n-hexane sensor is simple, and has no need of expensive instruments, which can be used for

RSC Advances Accepted Manuscript

safety control and air quality monitoring of the content of n-hexane in the workplace.

2. Experimental

2.1. Apparatus

The morphologies and microstructures of the catalysts were characterized by scanning electron microscopy (SEM, Hitachi S-4800). X-ray power diffraction (XRD) experiment was carried out with a Rigaku D/Max Ultima □ X-ray diffractometer using Cu Kα radiation at an acceleration voltage of 40 kV and a current of 40 mA. The XRD data are scanned from 10° to 90° with the step size of 0.02°. The schematic diagram of the sensing system was similar to our previous work (Fig. 1).[12] Minitab software was used for the optimizing and analyzing of the obtained data.

Fig. 1.

2.2. Chemicals and regents

Y_2O_3 was purchased from Shanghai Rich Joint Chemical Reagent CO., Ltd, China. γ-Al_2O_3 was purchased from Tianjin No.3 Chemical Reagent Factory, China. Tenax-TA, GC and GR 60/80 were purchased from CRS Company of America, and n-hexane (analytical grade) was purchased from Reagent Industry Company of East China, the glue used in the

RSC Advances Accepted Manuscript

107 preparation of sensing material was purchased from BoBo (YS-7001).

108 **2.3. Procedures**

109 A microsyringe was used to inject a certain volume of n-hexane (liquid
110 state) into a 30 L container, placed for 20 min to complete gasification to
111 simulate a certain concentration of n-hexane in air. Then, The adsorption
112 tube (containing 0.12 g Tenax-TA) was used to absorb n-hexane at room
113 temperature, desorbing the n-hexane adsorbed on surface of adsorbent by
114 heating up at the thermal desorption temperature. Then, the carrier air
115 took the desorbed n-hexane gas into the CTL chamber. Then n-hexane
116 vapor was oxidized on the surface of the chosen sensing material at a
117 certain temperature. Finally, the CTL intensity at a certain wavelength
118 was measured by a BPCL Ultra Weak Chemiluminescence Analyzer.

119 **2.4. Preparation of sensing material**

120 Powder materials of TiO_2, Y_2O_3, Y_2O_3-SiO_2 (mass ratio of 1:1),
121 Y_2O_3-Al_2O_3 (mass ratio of 3:1 and 2:1) and nanophase materials of Y_2O_3,
122 Fe_2O_3 and Cr_2O_3 were examined as sensing materials, by grounding with
123 mortar to make sure they mix well. 0.8 g of each material was weighed up.
124 The glue (about 0.1 mL) was coated on the surface of the ceramics
125 heating tube with a brush, and then the sensing material (with a thickness
126 of 0.5 mm) was wrapped around the above ceramics heating tube,
127 sintering the ceramics heating tube at 700 ^{o}C in the muffle for 2 h to
128 obtain the sensing material.

RSC Advances Accepted Manuscript

2.5. Experimental design and data analysis

As presented in Table 1, a central composite design (CCD) in the form of 2^3 full factorial design was used, in which three independent variables were converted to dimensionless ones (x_1, x_2, x_3),with the coded values at 3 levels: -1, 0, +1. The predicted response (y) was therefore correlated to the set of regression coefficients (β): the intercept (β_0), linear (β_1, β_2, β_3), interaction (β_{12}, β_{13}, β_{23}) and quadratic coefficient (β_{11}, β_{22}, β_{33}). Herein, the Minitab software was used for regression and graphical analyses of the obtain data.

$$y=\beta_0+\beta_1 x_1+\beta_2 x_2+\beta_3 x_3+\beta_{12}x_1x_2+\beta_{13}x_1x_3+\beta_{23}x_2x_3$$

Table 1.

3. Results and discussion

3.1. Characterization of sensing material

The morphology and structure of the catalysts were examined by SEM. Fig. 2 showed the sizes of Y_2O_3, Al_2O_3 were about 50 nm and 20 nm, respectively.

Fig. 2.

XRD results (Fig. 3) of the Y_2O_3/Al_2O_3 showed only peaks

RSC Advances Accepted Manuscript

corresponding to Y_2O_3 (highly crystalline C-type cubic Y_2O_3 , space group Ia3) but no crystalline bulk structures of interaction species involving yttria and alumina have been observed, as the low amorphous character of Al_2O_3 have not been deduced in the patterns. Results (Table 2) found that Y_2O_3-Al_2O_3 (mass ratio of 2:1) showed the highest CTL intensity and better selectivity to n-hexane than other materials. Herein, alumina may play a primary role in enhancing the yttria dispersion to against thermal sintering of the mixture.[30] On the other hand, Al_2O_3 induces a modification of the electronic density of the aluminum and lanthanide cations, implying a change in the acid–base properties of the support surface.[34-35]

Fig. 3

Table 2.

3.2. The CTL response profile

The CTL intensity on the surface of these materials was determined at a flow rate of 300 mL/min, wavelength of 400 nm, catalytic temperature (Tc) of 200 ^{o}C, thermal desorption temperature (Td) of 250 ^{o}C, thermal desorption time (td) of 480 s, and adsorbent of Tenax-TA. The CTL response profile of n-hexane on the surface of sensing material was

RSC Advances Accepted Manuscript

studied by injection of three different concentrations of n-hexane vapor. As can been seen from Fig. 4, The CTL signal increased with the concentration of n-hexane but the profiles were similar to each other. The peaks of each curve appeared at 4 s after sample injection, which showed that this sensor had a rapid response time, and the half decay time of CTL intensity of each curve was about 3 s.

Fig. 4.

3.3. Fitting the model

In this paper, response surface method (RSM) was used to find the optimal parameters of the actual test system. As the thermal radiation noise of ceramic heating tube increases with the increase of wavelength or temperature, signal to noise ratio (S/N) was used to represent the CTL intensity. In our experiments, the optimal conditions (for more details see ESI†) were the wavelength was at the minimum of 400 nm. So the parameters of thermal desorption temperature, thermal desorption time and flow rate were chosen to conduct response surface analysis and the simultaneous effect of the above parameters on CTL intensity was conducted (Fig 5). Herein, we take the simultaneous effect of thermal desorption temperature (Fig.5a) for example, the three-dimensional response surfaces which was constructed to illustrate the effects of the

RSC Advances Accepted Manuscript

thermal desorption temperature and chemical flow rate on the TCL intensity, showing the effect of the thermal desorption temperature and chemical flow rate showed significant effects on the response, namely, TCL intensity increased with increase of thermal desorption temperature from 220 to 250 ^{o}C, with a peak (higher than 8000 a.u.) at 250 ^{o}C and then decreased with the increase of temperature form 250 to 350 ^{o}C. As to chemical flow rate, the TCL intensity achieved the highest value (higher than 8000 a.u.) when the chemical flow rate was 300 mL/min. With the same analytical method to the data of the effect of thermal desorption time and flow rate (Fig.5b) and flow rate and thermal desorption temperature (Fig.5c) on the TCL intensity, in this experiment, the maximum TCL intensity (higher than 8000 a.u.) value was obtained at the parameter of the thermal desorption temperature of 250 ^{o}C, thermal desorption time of 480 s and flow rate of 300 mL/min. The statistical significance of the quadratic model was evaluated by the analysis of variance (ANOVA) as shown in Table 3, whose results revealed that this main effect was statistically significant at P-value of 0.000, which was smaller than the significant of 0.05, indicting high significant main effect of regression. Moreover, the lack off fit P-value was 0.517, indicting the regression equation was not lack off without the high order interaction effects.

RSC Advances Accepted Manuscript

Fig. 5.

Table 3.

The fit of the model was checked by the determination of coefficient (R^2). In this case, the value of the determination coefficient (R^2= 0.9996) indicated that only 0.04 % of the total variable was not explained by the model. The closer the R^2 is to 1, the stronger the model and the better it predicts the response. The value of adjusted determination coefficient (adjusted R^2 = 0.9987) is also high, showing a high significance of the model. The regression equation after the ANOVA gave the level of TCL intensity as a function of thermal desorption temperature, thermal desorption time and flow rate. By applying multiple regression analysis on the experimental data, the experimental results of the CCD design were fitted with a second-order full polynomial equation. The empirical relationship between TCL intensity (Y) and the three test variables in coded units obtained by the application of RSM is given by

$$Y=2451.50-3.525x_1-0.83889x_2+4.14333x_3+0.0018056x_1x_2+0.0221667x_1x_3+0.00591667x_2x_3$$

Minitab software was used for optimization and validation experiments, with the parameter of the thermal desorption temperature of 250 ^{o}C, thermal desorption time of 480 s and flow rate of 300 mL/min,

RSC Advances Accepted Manuscript

239 respectively. The optimal value of CTL intensity was 8109.67
240 (desirability of 0.442381) and the experiment average value was 8104.4
241 (n=5, RSD=1.23 %), in other words, the accuracy was 0.06 %. Through
242 the validation experiments of the software, there value of desirability
243 (95 %) showed that the value of the average of CTL intensity will fall in
244 the range of (8008.78, 8210.56) and the value of CTL intensity will fall in
245 the range of (7907.89, 8311.45), which was in agreement with the results
246 of the experiments (n=11).

247 **3.4. Interference studies**

248 The same concentration of n-hexane (6.59 mg/m^3) and the coexisted
249 foreign substance (such as benzene, toluene, dimethylbenzene,
250 formaldehyde, chloroform, ethanol, cyclohexane, methanol, acetaldehyde
251 or ammonia) were tested under the optimized conditions described above.
252 There was little to no response when contaminating volatile substances
253 including benzene, toluene, chloroform, ethanol, and cyclohexane is
254 passed though the sensor. In addition, when the concentrations of the
255 contaminating volatile substances were increased to 10 times, there was
256 also little to no response.

257 **3.5. Analytical characteristics**

258 Under the selected conditions describes above, the regression equation
259 of CTL intensity versus n-hexane vapor concentration was linear in the

RSC Advances Accepted Manuscript

range of 1.32-132 mg/m^3, with a detection limit of 0.4 mg/m^3. As shown in Fig. 6. The linear equation is I =707.86 C+1902.9 (r = 0.9976), where I is the relative CTL intensity, C is the concentration of n-hexane and r is correlation coefficient. The relative standard deviation (RSD, n = 11) is 5.88 % for 6.59 mg/m^3 n-hexane vapor.

Fig. 6.

3.6. Lifetime of the gas sensor

The sensor can continuously work for 100 h without significant decrease of the CTL intensity, which indicated the satisfactory stability and durability of the Y_2O_3-Al_2O_3 (mass ratio, 2:1) based sensor.

3.7. Sample analysis

In order to evaluate the validity of the proposed sensor for determination of n-hexane, classic thermal desorption gas chromatography (GBZ/T 160.38-2004) was carried out for comparison. The results are listed in Table 4, which was in agreement well with that obtained by gas chromatography.

RSC Advances Accepted Manuscript

Table 4.

In order to evaluate the analytical application of the proposed sensor for determination of n-hexane, three mixed samples containing known concentrations of n-hexane, formaldehyde, ammonia and benzene have been analyzed under the optimized conditions. As formaldehyde, ammonia and benzene are the common organic compounds which may coexist with n-hexane in air, they have been chosen in the mixed samples. To acquire the accurate analysis results, the calibration curve was under the same sampling condition as the sample analysis. As shown in Table 5, sample 1 and 2 was the mixture of n-hexane, formaldehyde and ammonia, sample 3 was a mixture of n-hexane, formaldehyde and benzene. And good selectivity was obtained in these three samples (Table 5).

Table 5.

4. Conclusions

In conclusion, the TD/CTL-based n-hexane sensor by using Y_2O_3-Al_2O_3 (mass ratio, 2:1) as sensing material has been proposed in this paper. By adding the TD, the sensitivity of the sensor is improved about 20 times, that is, with a lower detection limit of 0.4 mg/m^3

RSC Advances Accepted Manuscript

compared with that of without adding TD (8 mg/m^3). In addition, response surface methodology (RSM) was used to study the optimal conditions of the developed sensor for the determination of n-hexane and the results were in agreement with that of the experiments. The regression equation of TD/CTL intensity versus n-hexane vapor concentration is linear in the range of 1.32-132 mg/m^3, which demonstrates that TD/CTL shows a higher sensitivity and a better selectivity. The TD/CTL-based sensor proposed here has the unique properties of high sensitivity rapid response and satisfactory durability, indicating that this kind of sensor will have a bright future for various VOCs determination in environmental monitoring.

Acknowledgement

This work was supported by the National Natural Science Foundation of China (No. 40506020, 20775067, 20977074, and 21175115, S. X. L), the Program for New Century Excellent Talents in University (NCET-11 0904, S. X. L), Outstanding Youth Science Foundation of Fujian Province, China (No. 2010J06005, S. X. L), and Natural Science Foundation of Fujian province in China (2012Y0065, F. Y. Z).

RSC Advances Accepted Manuscript

References

1 G. Kutlu, Y. B. Gonceli, T. Sonmez and L. E. Inan, J. Clin. Neurosci, 2009, **16**, 1296-1299.

2 C. M. Chang, C. W. Yu, K. Y. Fong, S. Y. Leung, T. W. Tsin, Y. L. Yu, T. F. Cheung and S. Y. Chan, Neurol Neurosurg Psychiatry, 1993, **56**, 538-542.

3 S. Abe, T. Okutsu, H. Nakajima, N. Kakuda, I. Ohtsu and R. Aono, Microbiology, 2003, **149**, 1265-1273.

4 S. Sanagi, Y. Seki, K. Sugimoto and M. Hirata, International Archives of Occupational and Environmental Health, 1980, **47**, 69-79.

5 M. J. Prieto-Castelló, M. L. Hernández-Viadel, A. Cardona and D. Marhuenda, Toxico- logy, 2007, **229**, 73-78.

6 M. J. Prieto, D. Marhuenda, J. Roel and A. Cardona, Toxicol. Lett., 2003, **145**, 249-260.

7 C. N. Konidari, C. D. Stalikas and M. I. Karayannis, Anal. Chim. Acta, 2001, **442**, 231-239.

8 B. K. Zhu, H. L. Deng and X. M. Chen, Trop. Med., 2006, **6**, 1659-1660.

9 Z. Z. Ke, X. L. Yu, X. Y. Xie, X. Lin, J. G. Chen and Z. Y. Wang, J. Prev. Med., 2003, **9**, 57-58 (in Chinese).

10 S. F. Li, F. P. Li and Z. M. Rao, Sens. Actuators B, 2010, **145**, 78-83.

11 J. Z. Zheng, S. F. Li, W. X. Zhang, J. Cao, S. X. Li and Z. M. Rao,

RSC Advances Accepted Manuscript

Analyst, 2013, **138**, 916-920.

12 J. Z. Zheng, Z. J. Xue, S. F. Li, S. X. Li and Z. M. Rao, Analytical Methods, 2012, **4**, 2791-2796.

13 P. Yang, X. N. Ye, C. W. Lau, Z. X. Li, X. Liu and J. Z. Lu, Anal. Chem., 2007, **79**, 1425-1432.

14 P. Yang, C. W. Lau, X. Liu and J. Z. Lu, Anal. Chem., 2007, **79**, 8476-8485.

15 X. A. Cao, G. M. Feng, H. H. Gao, X. Q. Luo and H. L. Lu, Luminescence, 2005, **20**, 104-108.

16 J. S. Lu, X. A. Cao, C.Y. Pan, L. F. Yang, G. B. Lai, J. L. Chen and C. Q. Wu, Sensors, 2006, **6**, 1827-1836.

17 L. Tang, Y. M. Li, K. L. Xu, X. D. Hou and Y. Lv, Sens. Actuators B, 2008, **132**, 243-249.

18 Y. Y. Wu, S. C. Zhang, X. Wang, N. Na and Z. X. Zhang, Luminescence, 2008, **23**, 376-380.

19 Z. M. Rao, L. J. Liu, J. Y. Xie and Y. Y. Zeng, Luminescence, 2008, **23**, 163-168.

20 Z. Y. Zheng, K. Xu, W. R. G. Baeyens and X. R. Zhang, Anal. Chim. Acta, 2005, **535**, 145-152.

21 C. Yu, G. H. Liu, B. L. Zuo, Y. J. Tang and T. Zhang, Anal. Chim. Acta, 2008, **618**, 204-209.

RSC Advances Accepted Manuscript

22 Y. L. Xuan, J. Hu, K. L. Xu, X. D. Hou and Y. Lv, Sens. Actuators B, 2009, **136**, 218-223.

23 X. A. Cao, W. F. Wu, N. Chen, Y. Peng and Y. H. Liu, Sens. Actuators B, 2009, **137**, 83-87.

24 L. Luo, H. Chen, L. C. Zhang, K. L. Xu and Y. Lv, Anal. Chim. Acta, 2009, **635**, 183-187.

25 C. C. Wu, X. A. Cao, Q. Wen, Z. H. Wang, Q. Q. Gao and H. C. Zhu, Talanta, 2009, **79**, 1223-1227.

26 E. D. Park and J. S. Lee, J. Catal., 1999, **186**, 1-11.

27 P. A. Sermon, G. C. Bond, P. B. Wells and Faraday Trans., 1979, **75**, 385-394.

28 I. A. W. Tan, A. L. Ahmad and B. H. Hameed, Chem Eng J., 2008, **137**, 462-470.

29 D. Baş and I. H. Boyacı, J FOOD ENG, 2007, **78**, 836–845.

30 M. Amini, H. Younesi, N. Bahramifar, A. A. Z. Lorestani, F. Ghorbani, A. Daneshi and M. Sharifzadeh, J. Hazard. Mater., 2008, **154**, 694-702.

31 A. Ueda and M. Haruta, Appl. Catal. B, 1998, **18**, 115-121.

32 F. Porta, L. Prati, M. Rossi, S. Coluccia and G. Martra, Catal. Today, 2000, **61**, 165-172.

33 R. Dictor and S. Roberts, J. Phys. Chem., 1989, **93**, 5846-5850.

34 M. A. Centeno, P. Malet, I. Carrizosa and J. A. Odriozola, J. Phys.

RSC Advances Accepted Manuscript

Chem. B, 2000, **104**, 3310-3319.

35 A. Borgna, T. F. Garetto and C. R. Apesteguia, Appl. Catal. A, 2000, **197**, 11-21.

RSC Advances Accepted Manuscript

Figure captions

Fig. 1 Schematic diagram of the TD/CTL sensing system.

Fig. 2 SEM images of (a) Y_2O_3 and (b) Al_2O_3.

Fig. 3 X-ray powder diffraction pattern of Y_2O_3-Al_2O_3 (mass ratio of 2:1).

Fig. 4 CTL response profiles of three different concentrations of n-hexane vapor (400 nm, Tc: 200 ^oC, Td: 250 ^oC, td: 480 s, Tenax-TA).

Fig. 5 Response surface plots for the effect of (a) thermal desorption temperature (^oC) and thermal desorption time (s); (b) thermal desorption temperature (^oC) and flow rate (mL/min); (c) thermal desorption time (s) and flow rate (mL/min).

Fig. 6 The calibration curve for n-hexane.

Table captions

Table 1. Experimental ranges and levels of the independent variables.

Table 2. The CTL intensity of n-hexane on the surface of different materials.

Table 3. Regression analysis using the 2^3 factorial central composite design.

RSC Advances Accepted Manuscript

427 **Table 4.** The on-line analyses of n-hexane vapor samples.

428 **Table 5.** The analysis of n-hexane vapour samples.

429

RSC Advances Accepted Manuscript

Figure captions

Fig. 1 Schematic diagram of the TD/CTL sensing system.

Fig. 2 SEM images of (a) Y_2O_3 and (b) Al_2O_3.

Fig. 3 X-ray powder diffraction pattern of Y_2O_3-Al_2O_3 (mass ratio of 2:1).

Fig. 4 CTL response profiles of three different concentrations of n-hexane vapor (400 nm, Tc: 200 ^oC, Td: 250 ^oC, td: 480 s, Tenax-TA).

Fig. 5 Response surface plots for the effect of (a) thermal desorption temperature (^oC) and thermal desorption time (s); (b) thermal desorption temperature (^oC) and flow rate (mL/min); (c) thermal desorption time (s) and flow rate (mL/min).

Fig. 6 The calibration curve for n-hexane.

RSC Advances Accepted Manuscript

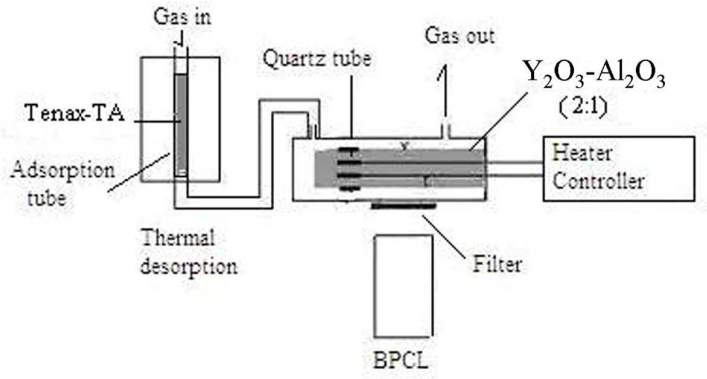

Fig. 1 Schematic diagram of the TD/CTL sensing system.

RSC Advances Accepted Manuscript

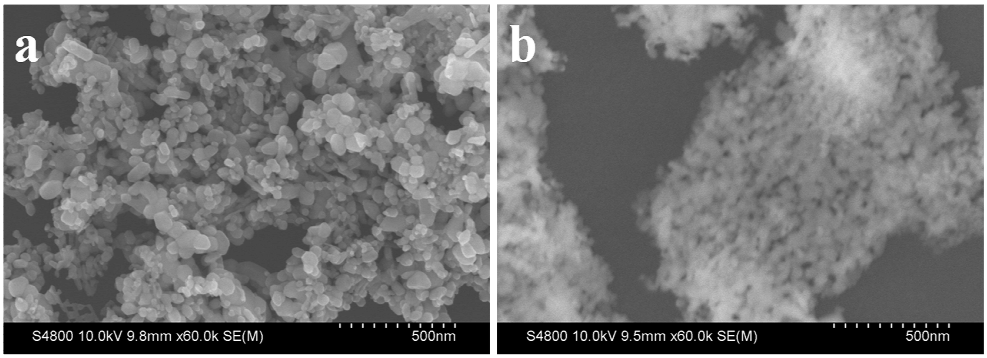

Fig. 2 SEM images of (a) Y_2O_3 and (b) Al_2O_3.

RSC Advances Accepted Manuscript

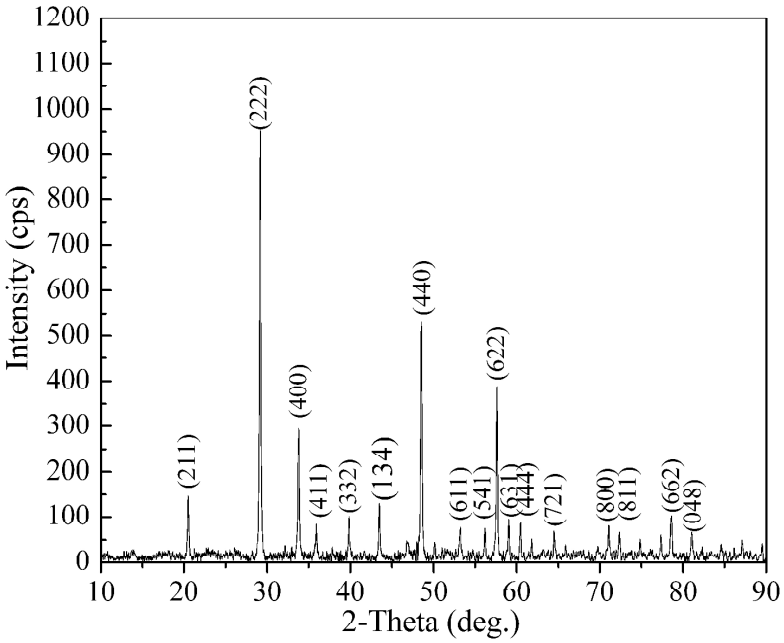

Fig. 3 X-ray powder diffraction pattern of Y_2O_3-Al_2O_3 (mass ratio of 2:1).

RSC Advances Accepted Manuscript

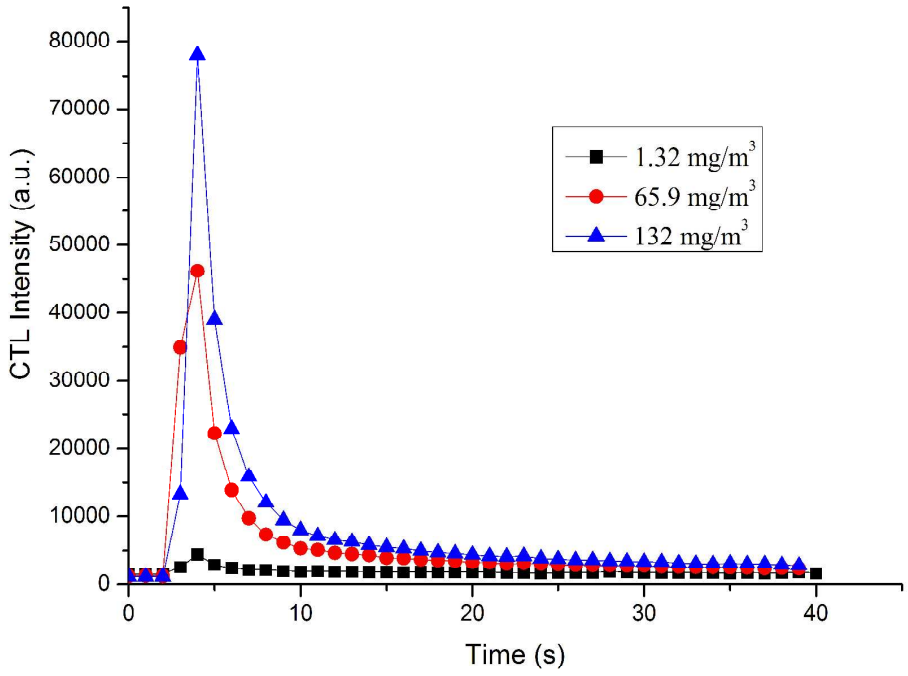

Fig. 4 CTL response profiles of three different concentrations of n-hexane vapor (400 nm, Tc: 200 ^{o}C, Td: 250 ^{o}C, td: 480 s, Tenax-TA).

RSC Advances Accepted Manuscript

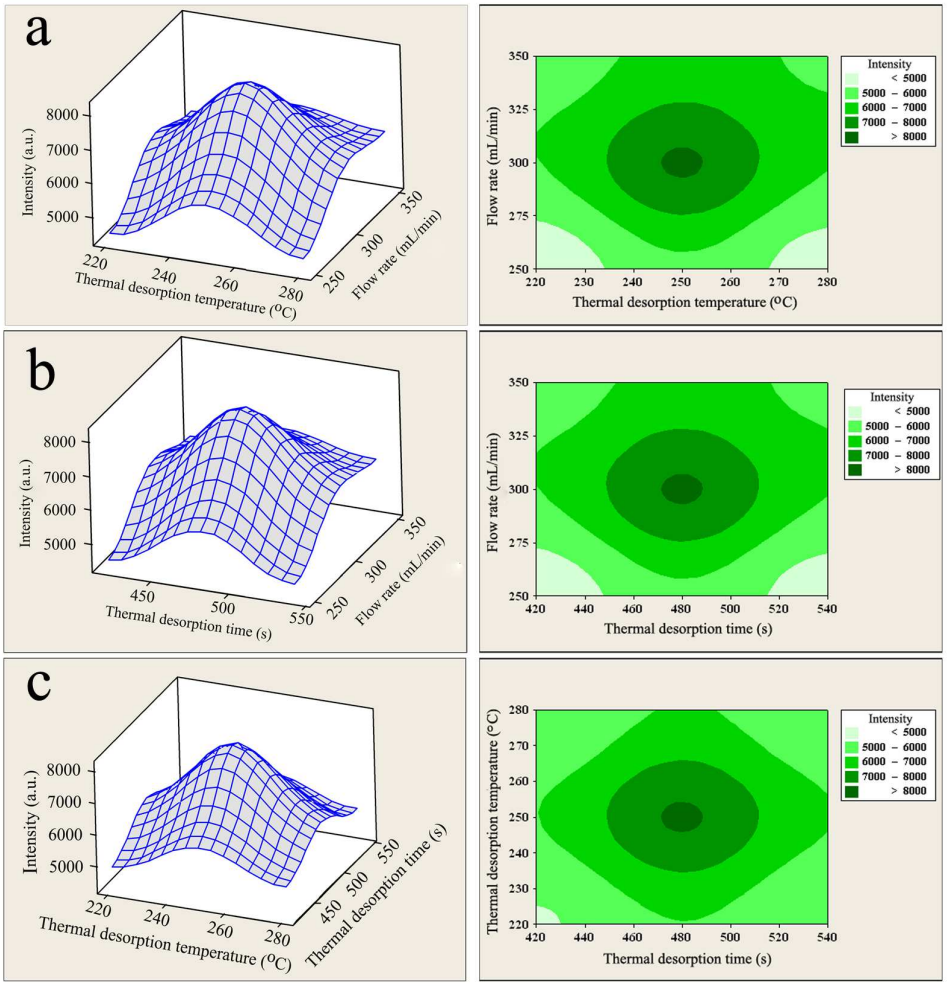

Fig. 5 Response surface plots for the effect of (a) thermal desorption temperature (°C) and thermal desorption time (s); (b) thermal desorption temperature (°C) and flow rate (mL/min); (c) thermal desorption time (s) and flow rate (mL/min).

RSC Advances Accepted Manuscript

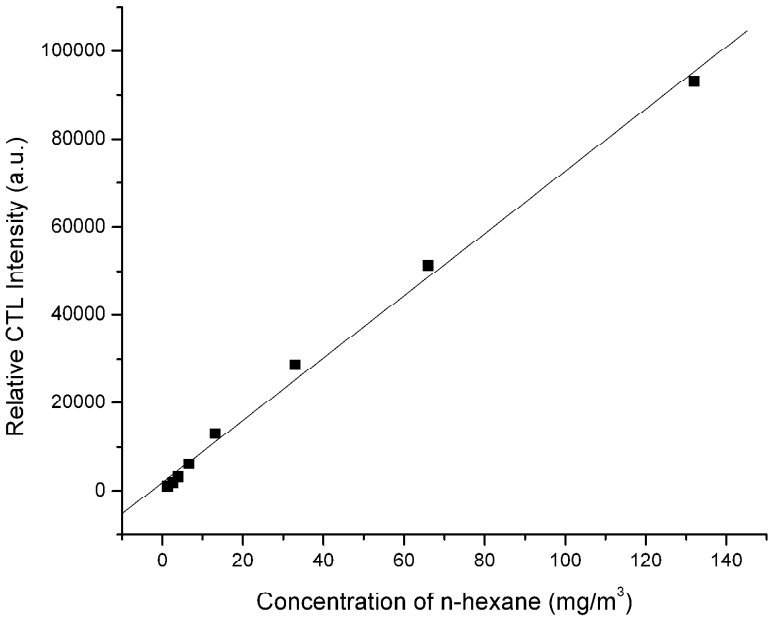

Fig. 6 The calibration curve for n-hexane.

RSC Advances Accepted Manuscript

Table captions

Table 1. Experimental ranges and levels of the independent variables.

Table 2. The CTL intensity of n-hexane on the surface of different materials.

Table 3. Regression analysis using the 2^3factorial central composite design.

Table 4. The on-line analysis of n-hexane vapour samples.

Table 5. The analysis of n-hexane vapour samples.

RSC Advances Accepted Manuscript

Table 1. Experimental ranges and levels of the independent variables.

Independent variables	Range and level		
	-1	0	1
Thermal desorption temperature (^{o}C) (x_1)	220	250	280
Thermal desorption time (s) (x_2)	420	480	540
Flow rate (mL min^{-1}) (x_3)	250	300	350

RSC Advances Accepted Manuscript

Table 2. The CTL intensity of n-hexane on the surface of different materials.

Materials (mass ratio)	Y_2O_3-Al_2O_3 (3:1)	Nano-Cr_2O_3	Y_2O_3	Y_2O_3-SiO_2 (1:1)	Y_2O_3-Al_2O_3 (2:1)	Nano-Y_2O_3	TiO_2	Y_2O_3-SiO_2 (3:1)	Nano-Fe_2O_3
S/N	2.53	0	2.84	2.43	5.92	2.57	0	2.41	0

RSC Advances Accepted Manuscript

Table 3. Regression analysis using the 2^3factorial central composite design.

Model term	effect	Coefficient estimate	F-Value	p-Value
Intercept		5141.75	264.86	0.000
x_1	239.50	119.75	6.17	0.009
x_2	166.50	83.25	4.29	0.023
x_3	1252.50	626.25	32.26	0.000
x_1*x_2	6.50	3.25	0.17	0.031
x_1*x_3	66.50	33.25	1.71	0.018
x_2*x_3	35.50	17.75	0.91	0.024

RSC Advances Accepted Manuscript

Table 4. The on-line analysis of n-hexane vapour samples.

Sample No.	TCL method (mg/m^3, n=5)	RSD (%, n = 5)	GC Standard methods (mg/m^3, n=5)	RSD (%, n = 5)
1	3.96	3.42	4.06	4.33
2	6.59	2.78	6.48	3.22
3	21.76	4.75	21.93	3.16

RSC Advances Accepted Manuscript

Table 5. The analysis of n-hexane vapour samples.

Sample No.	Composition	Standard values (mg/m^3)	Measured values (mg/m^3, n=5)	n-Hexane Recovery (%)
1	n-Hexane	21.97	21.24 ± 0.48	96.70
	Formaldehyde	1.29		
	Ammonia	0.73		
2	n-Hexane	21.97	21.47 ± 0.53	97.72
	Formaldehyde	2.58		
	Ammonia	1.46		
3	n-Hexane	21.97	20.03 ± 1.20	91.12
	Formaldehyde	1.29		
	Benzene	2.93		

RSC Advances Accepted Manuscript